Magnetosphere inflation during the recovery phase of geomagnetic storms as an excellent magnetic confinement of killer electrons

Ryuho Kataoka[1] and Yoshizumi Miyoshi[2]

Received 29 August 2007; revised 13 October 2007; accepted 9 November 2007; published 7 February 2008.

[1] Extreme flux enhancement of outer radiation belt electrons was observed at geosynchronous orbit during the recovery phase of a large magnetic storm on 27–30 July 2004. The storm main phase is driven by a very fast magnetic cloud of ~1000 km/s associated with a coronal mass ejection (CME). The high-speed stream of ~600 km/s originated from a coronal hole follows the magnetic cloud and the coronal hole stream (CHS) is rarefied due to the speed difference between the CME and CHS. During the storm recovery phase, the magnetosphere is surrounded by the very low-density CHS, causing an inflation of the magnetosphere. It is found that such a combination of the CME and CHS can be one of the most dangerous solar wind structures for the outer radiation belt, and the associated very low dynamic pressure can cause the magnetosphere inflation during the storm recovery phase as an excellent magnetic confinement of killer electrons. **Citation:** Kataoka, R., and Y. Miyoshi (2008), Magnetosphere inflation during the recovery phase of geomagnetic storms as an excellent magnetic confinement of killer electrons, *Geophys. Res. Lett.*, *35*, L06S09, doi:10.1029/2007GL031842.

1. Introduction

[2] One of the most important problems for space weather study is to understand how to predict the extreme flux enhancement of "killer electrons" in the Van Allen radiation belts. *Miyoshi and Kataoka* [2005] showed evidence that the relativistic electron flux enhancement at geosynchronous orbit during isolated geomagnetic storms is, on average, significantly stronger in the storms driven by corotating interaction regions (CIRs) than in storms driven by coronal mass ejections (CMEs). The obtained average profiles of the isolated CIR- and CME-driven storms are actually helpful and especially useful to predict the daily probability variation of the outer belt flux alert [*Kataoka and Miyoshi*, 2006; *Miyoshi and Kataoka*, 2008a, 2008b]. However, such an average picture for isolated storms sometimes does not work well to predict the extreme events when multiple storms occur within a few days and/or the storms are driven by complex solar wind structures. This brief report addresses the problem to provide a complementary understanding how to predict the most dangerous situation at geosynchronous orbit driven by a complex solar wind structure, focusing on the July 2004 storm events when the GOES satellites at geosynchronous orbit observed the largest relativistic electron flux during solar cycle 23.

[3] Some extreme events are associated with magnetosphere compression during super storms driven by CMEs. For example, one of the famous extreme events of the radiation belts is associated with a strong interplanetary shock impacting the magnetosphere [*Blake et al.*, 1992; *Li et al.*, 1993]. *Baker et al.* [2004] also reported a different type of extreme event that the slot region and inner radiation belt was extremely enhanced during the Halloween 2003 super storm. In this paper, we suggest a new mechanism of extreme flux enhancement at geosynchronous orbit due to the magnetosphere inflation during the storm recovery phase associated with the combination of CMEs and high-speed solar wind stream originated from coronal holes.

2. Extreme Event

[4] First of all, three intense storms occurred during the last week in July 2004 as shown in Figure 1g. The interplanetary drivers of these storms are basically magnetic clouds associated with halo-type CMEs: The magnetic cloud properties can be identified in Figures 1a, 1b, and 1e by the interplanetary magnetic field (IMF) stronger than average, smoothly rotating IMF, and very low proton temperature [*Burlaga et al.*, 1981], respectively. The reference temperature is calculated as an empirical function of the solar wind speed [*Lopez*, 1987] and is shown by the red line in Figure 1e. The most unusual discontinuous feature found in Figure 1 is the sudden drop in the solar wind speed at ~0200 UT on 28 July (total day 210), as shown by vertical dashed line. The velocity shear corresponds to a heliospheric current sheet as identified by the rapid change in the azimuth direction of the IMF (Figure 1b). The discontinuity plays a role as an interface separating the CME material and the high-speed stream of ~600 km/s originated from a coronal hole. After the discontinuity, the solar wind parameters show typical values as a coronal hole stream (CHS) [*Kataoka and Miyoshi*, 2006], except for the very low density of less than 1.0/cc. Figure 2 shows the SOHO/EIT 284 nm image, indicating the relative location of the low-latitude coronal hole in the southern hemisphere and the active region associated with the halo CMEs. The coronal hole has a toward magnetic field polarity, consistent with the sector polarity shown in Figure 1b.

[5] GOES satellites at geosynchronous orbit observed extremely large flux enhancement of >2.0 MeV electrons for total day 210–212 (Figure 3a) when the solar wind dynamic pressure was less than 1.0 nPa (Figure 1d). The peak flux value exceeds 10^5/cm^2 sec str, and this is the largest event during solar cycle 23. As a reference, top ten

[1]RIKEN, Wako, Japan.
[2]Solar-Terrestrial Environment Laboratory, Nagoya University, Nagoya, Japan.

Copyright 2008 by the American Geophysical Union.
0094-8276/08/2007GL031842

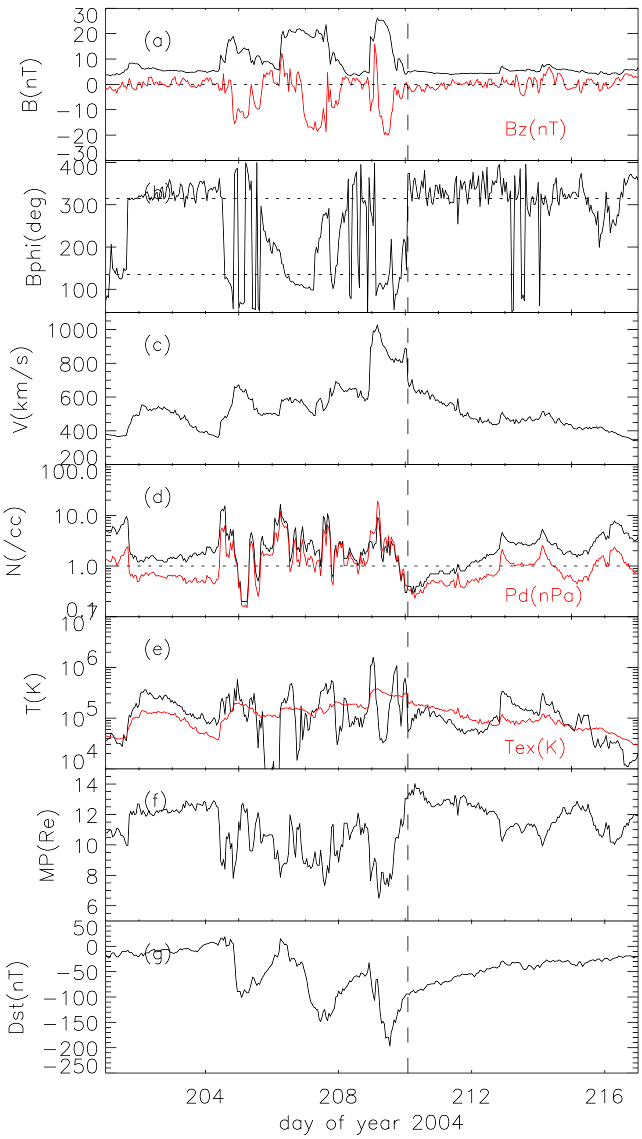

Figure 1. Solar wind parameters and provisional Dst index for the 16 day interval from 19 July to 4 August 2004 (total day 201–217). (a) Interplanetary magnetic field strength B and the southward component Bz in the GSM coordinate system, (b) azimuth angle of the magnetic field Bphi, (c) solar wind speed V, (d) proton number density N and dynamic pressure Pd, (e) proton temperature T and expected temperature Tex [*Lopez*, 1987], (f) subsolar magnetopause distance MP [*Shue et al.*, 1998], and (g) the provisional Dst index. The vertical dashed line indicates the heliospheric current sheet separating the magnetic cloud material and coronal hole stream.

events during solar cycle 23 are summarized in Table 1. As shown in Figure 3b, the daily variation of the GOES magnetic field Hp component, vertical to the orbital plane, is significantly smaller than usual for the total day 210–212, suggesting that the magnetic field configuration is more dipole-like than usual due to the inflation of the magnetosphere. In fact, according to an empirical model [*Shue et al.*, 1998], the magnetopause distance at the subsolar point expands even up to a nominal bow shock distance of ~13 Re.

[6] The spatial variation of the outer belt can be investigated using NOAA/POES MEPED observations [*Evans and Greer*, 2000]. As shown in Figure 4, the extreme flux enhancement for the total day 210–212 corresponds to the outward expansion of the outer belt over geosynchronous orbit. Also, the outer belt shows gradual inward (close to the Earth) expansion from the beginning of the storms (total day 205) to the end (total day 217). The flux peak appeared at L ~ 3 for the total day 210–212, far inside the geosynchronous orbit.

3. Summary and Discussion

[7] The extreme flux enhancement of >2.0 MeV electrons was observed at geosynchronous orbit (Figure 3a). The interplanetary cause was a very low density CHS connected to the trailing part of a much faster CME (Figure 1). The strongly southward IMF embedded in the CME material caused the storm main phase, and the magnetosphere was surrounded by the low-density CHS during the storm recovery phase. As a result of the low dynamic pressure during the recovery phase, the magnetosphere expanded (Figure 1f) and the magnetic field configuration became more dipole-like than usual (Figure 3b), causing the outer belt expansion over the geosynchronous orbit (Figure 4).

[8] The above observations can be explained as follows: In the inflated dipole-like magnetosphere, the trapping region of energetic particles expands outward to significantly reduce the drift loss process at the magnetopause, and to set an idealized natural accelerator with an excellent magnetic confinement of the energetic particles. Since the acceleration process of energetic particles was already ignited in the inner magnetosphere during the recovery phase, the outer belt can be widely distributed and expands outward than usual.

[9] It is apparent that only the very low dynamic pressure is not a sufficient condition to produce the extreme event as can be seen for total day 203–204 for instance: Magnetosphere inflation due to the low dynamic pressure can be identified (Figures 1d and 3b), and the geosynchronous flux was actually enhanced but not extremely at all possibly because of the lack of storms. In fact, we do not observe the extreme flux enhancement even during the famous day the solar wind disappeared in May 1999 [e.g., *Richardson et al.*, 2000], again possibly because of the lack of storms. Some strong acceleration processes associated with storms may be needed before or at the same time of the magnetosphere inflation to produce the extreme event at geosynchronous orbit. Also, a rapid expansion of the trapping boundary over the geosynchronous orbit at the early recovery phase may be important to produce the extreme event.

[10] Generally speaking, CIR and following high-speed CHS are an effective solar wind structure to enhance the outer belt flux typically associated with the high-intensity long-duration continuous AE activities (HILDCAAs) [*Tsurutani and Gonzalez*, 1987], while fast CMEs are not necessary highly effective to enhance the outer belt flux as shown by *Miyoshi and Kataoka* [2005]. In the present case, the HILDCAAs is not involved in the flux enhancement, suggesting that the flux enhancement occurs in a different way from the scenario working in usual CIR storms [*Miyoshi and Kataoka*, 2005; *Miyoshi et al.*, 2007].

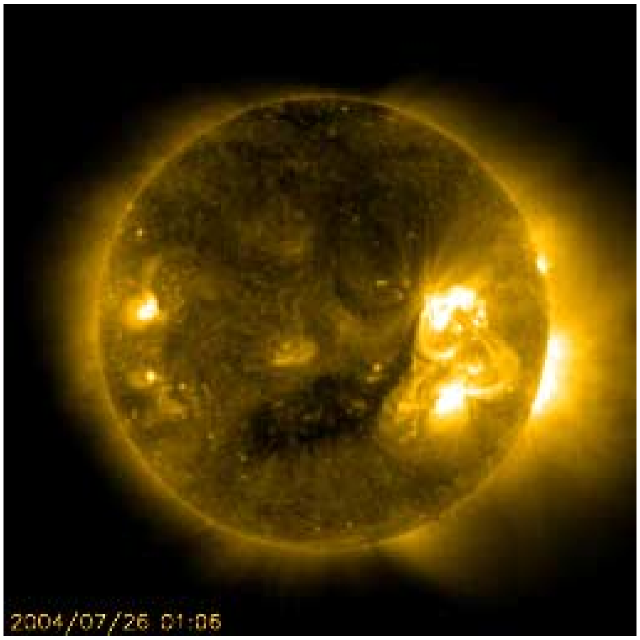

Figure 2. SOHO EIT 284 nm image on 26 July 2004 (total day 208). The coronal hole located over the central meridian in the southern hemisphere, and the active regions associated with the halo CMEs located at westside of the coronal hole.

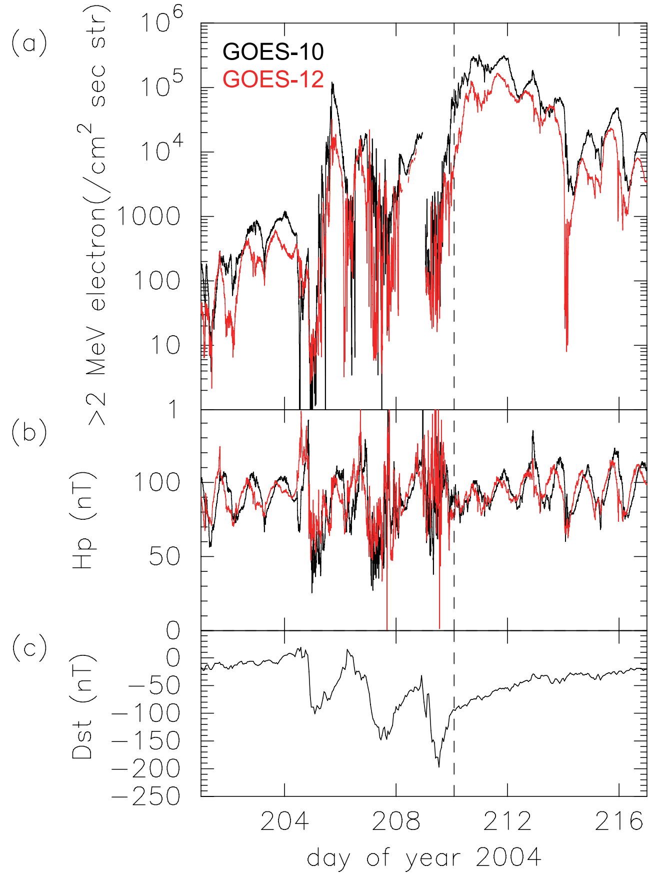

Figure 3. The GOES satellite observation of (a) >2.0 MeV electron flux, (b) magnetic field component Hp, and (c) the provisional Dst index, for the same time interval of Figure 1. In order to avoid any contaminations from the solar protons, the electron data are not presented when the flux of the 9–15 MeV proton sensor is larger than 10 /cm^2 sec str. The vertical dashed line indicates the arrival time of heliospheric current sheet as shown in Figure 1.

In fact, the NOAA/POES did not observe continuous injections of hot electrons from the plasma sheet during the recover phase (not shown). In this paper we suggest a new combined type of solar wind structure, the fast CME and following CHS, to produce the extreme enhancement: Fast CMEs tend to produce the main phase of intense storms [e.g., *Kataoka et al.*, 2005]. When the fast CME have a higher speed than following CHS, the CHS is rarefied by the fast CME. Since the CHS originally has a low density than average, the rarefied CHS has an extremely low density, and therefore the magnetopause is unusually expanded due to the very low dynamic pressure during the recovery phase.

[11] Such a situation does not occur so frequently because fast CMEs tend to occur during solar maxima when coronal holes tend to disappear, and coronal holes tend to occur during solar minima when fast CMEs tend to disappear. The declining phase of the solar cycle may be a reasonable time to produce such a combined type of solar wind structure due to the overlap occurrence of coronal holes and fast CMEs.

[12] As shown in right three columns of Table 1, the extreme events tend to occur when the dynamic pressure stays at low value of <1.0 nPa for a few days during the storm recovery phase in association with the CHS. From Table 1, it is found that there are several types of solar wind structures other than the combined structure of fast CME and CHS to produce the very low dynamic pressure during the storm recovery phase. Although this is beyond the scope of this paper, in future work, it would be important for space weather forecast study to understand the general cause of the very low dynamic pressure in the solar wind over multiple solar cycles, and to understand the inflated magnetosphere during the storm recovery phase as a natural accelerator with an excellent magnetic confinement of killer electrons.

Table 1. List of Top 10 Extreme Flux Enhancement[a]

Ranking	Max. Flux	Year	Month	Day	Total Day	Pd < 1.0 nPa	Rec. Phase	CHS
1	5.223	2004	7	29	211	yes	yes	yes
2	4.936	2005	5	18	138	yes	yes	no
3	4.876	2005	9	19	262	yes	yes	not clear
4	4.719	2006	4	17	107	yes	yes	yes
5	4.691	2005	8	9	221	yes	yes	yes
6	4.689	2004	2	18	49	yes	yes	yes
7	4.674	2004	11	11	316	no	yes	no
8	4.660	2006	12	15	349	yes	yes	no
9	4.629	2003	9	20	263	yes	yes	yes
10	4.590	2005	9	5	248	yes	yes	not clear

[a]The data source is >2.0 MeV electron flux observed by GOES 8 or GOES 12 satellites during solar cycle 23. The time period from May 2003 to August 2003 is not included due to the observation data gap. The maximum flux is in unit of log 10 (/cm^2 sec str).

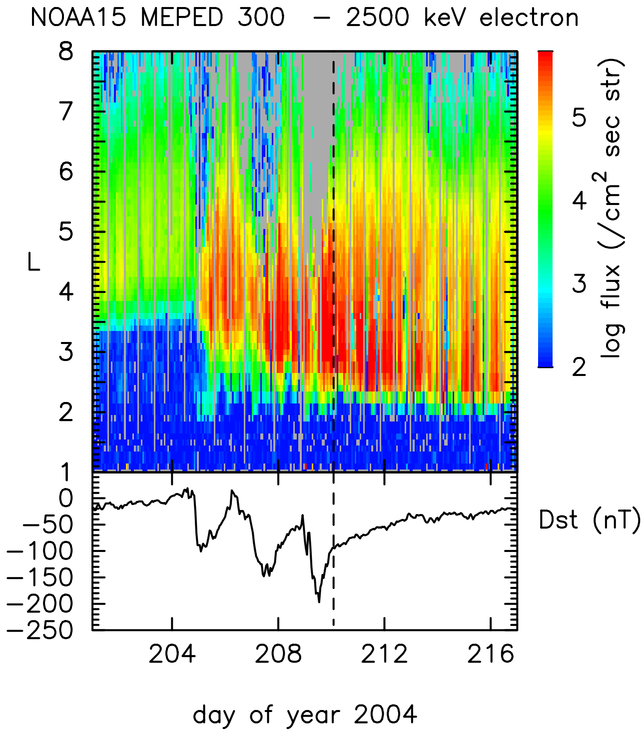

Figure 4. The NOAA/POES 15 MEPED observation of trapped electrons in the energy range of 300–2500 keV for the same time interval of Figure 1. The L-value is McIlwain's L derived from IGRF. In order to avoid any contamination from the energetic protons, the electron data are not used when the electron flux of the NOAA/MEPED 300–2500 keV sensor is less than ten times of the ion flux of the NOAA/MEPED 240–800 keV sensor, as shown by Gray regions. The provisional Dst index is also shown at bottom for reference. The vertical dashed line indicates the arrival time of heliospheric current sheet as shown in Figure 1.

[13] **Acknowledgments.** We thank the project teams providing their data: The POES and GOES data are provided from NOAA, the solar wind data are provided from OMNI2, the solar image data are provided from SOHO/EIT, and the provisional Dst index is provided from Kyoto University. The work by RK is supported by RIKEN Special Postdoctoral Research Fellowship.

References

Baker, D. N., S. G. Kanekal, X. Li, S. P. Monk, J. Goldstein, and J. L. Burch (2004), An extreme distortion of the Van Allen belt arising from the 'Halloween' solar storm in 2003, *Nature*, *423*, 878–881.

Blake, J. B., W. A. Kolasinski, R. W. Fillius, and E. G. Mullen (1992), Injection of electrons and protons with energies of tens of MeV into L less than 3 on 24 March 1991, *Geophys. Res. Lett.*, *19*, 821–824.

Burlaga, L. F., E. Sittler, F. Mariani, and R. Schwenn (1981), Magnetic loop behind an interplanetary shock: Voyager, Helios and IMP-8 observations, *J. Geophys. Res.*, *86*, 6673–6684.

Evans, D. S., and M. S. Greer (2000), Polar orbiting environmental satellite space environment monitor: 2. Instrument description and archive data documentation, *Tech. Memo. OAR SEC-93*, NOAA, Boulder, Colo.

Kataoka, R., and Y. Miyoshi (2006), Flux enhancement of radiation belt electrons during geomagnetic storms driven by coronal mass ejections and corotating interaction regions, *Space Weather*, *4*, S09004, doi:10.1029/2005SW000211.

Kataoka, R., S. Watari, N. Shimada, H. Shimazu, and K. Marubashi (2005), Downstream structures of interplanetary fast shocks associated with coronal mass ejections, *Geophys. Res. Lett.*, *32*, L12103, doi:10.1029/2005GL022777.

Li, X., I. Roth, M. Temerin, J. R. Wygant, M. K. Hudson, and J. B. Blake (1993), Simulation of the prompt energization and transport of radiation particles during the March 24, 1991 SSC, *Geophys. Res. Lett.*, *20*, 2423–2426.

Lopez, R. E. (1987), Solar cycle invariance in the solar wind proton temperature relationships, *J. Geophys. Res.*, *92*, 11,189–11,194.

Miyoshi, Y., and R. Kataoka (2005), Ring current ions and radiation belt electrons during geomagnetic storms driven by coronal mass ejections and corotating interaction regions, *Geophys. Res. Lett.*, *32*, L21105, doi:10.1029/2005GL024590.

Miyoshi, Y., and R. Kataoka (2008a), Flux enhancement of the outer radiation belt electrons associated with stream interaction regions, *J. Geophys. Res.*, *113*, A03S09, doi:10.1029/2007JA012506.

Miyoshi, Y., and R. Kataoka (2008b), Probabilistic space weather forecast of the relativistic electron flux enhancement at geosynchronous orbit, *J. Atmos. Sol. Terr. Phys*, in press.

Miyoshi, Y., A. Morioka, R. Kataoka, Y. Kasahara, and T. Mukai (2007), Evolution of the outer radiation belt during the November 1993 storms driven by corotating interaction regions, *J. Geophys. Res.*, *112*, A05210, doi:10.1029/2006JA012148.

Richardson, I. G., D. Berdichevsky, M. D. Desch, and C. J. Farrugia (2000), Solar-cycle variation of low density solar wind during more than three solar cycles, *Geophys. Res. Lett.*, *27*, 3761–3764.

Shue, J.-H., et al. (1998), Magnetopause location under extreme solar wind conditions, *J. Geophys. Res.*, *103*, 17,691–17,700, doi:10.1029/98JA01103.

Tsurutani, B. T., and W. D. Gonzalez (1987), The cause of high-intensity long-duration continuous AE activity (HILDCAAs): Interplanetary Alfven wave trains, *Planet. Space Sci.*, *35*, 305–412.

R. Kataoka, RIKEN, 2-1, Hirosawa, Wako, Saitama, 351-0198, Japan. (ryuho@riken.jp)

Y. Miyoshi, Solar-Terrestrial Environment Laboratory, Nagoya University, Furo-cho, Nagoya 464-8601, Japan. (miyoshi@stelab.nagoya-u.ac.jp)